www.czasopisma.pan.pl PAN POLSKA AKADEMIA NAUK www.journals.pan.pl

Arch. Metall. Mater. **66** (2021), 3, 729-733

DOI: 10.24425/amm.2021.136370

SUHWAN YOO[1], JUNG-MIN OH[1], JAEYEOL YANG[2], JAESIK YOON[2], JAE-WON LIM[1*]

EFFECT OF IMPURITY REDUCTION ON MECHANICAL PROPERTIES OF $Fe_{29.5}Ti_{70.5}$ ALLOY PREPARED BY PRETREATED Ti SCRAPS

Ferrotitanium can be produced as a method of recycling Ti scraps. The eutectic composition of ferrotitanium, $Fe_{29.5}Ti_{70.5}$, can be obtained as a nanocrystalline phase due to relatively low melting point. $Fe_{29.5}Ti_{70.5}$ in which FeTi and β-Ti form a lamellar structure have high strength but low strain. To improve this, impurities were removed through hydrogen plasma arc melting (HPAM) and annealed. HPAM can remove substitutional/interstitial solid solutions. As a result, from 6733 ppm to 4573 ppm of initial impurities were removed by HPAM process. In addition, the strain was improved by spheroidizing and coarsening the lamellar structure through annealing. The effect of impurities removed through HPAM on the Young's modulus, yield strength, and strain was observed.

Keywords: Ti scraps, Pre-treatment, Recycling, Refining

1. Introduction

The production of ferrotitanium is one of the approaches to recycle Ti scraps. When ferrotitanium is used as a structural agent, it is an alloy near the composition of the eutectic and forms a fine lamellar structure owing to its relatively low melting point. It has a high strength and excellent abrasion characteristics compared to those of coarse-grained materials. However, ultrafine eutectic alloys have limited strains at room temperature, which hinders their industrial applications as structural materials [1,2].

Ti scraps contain impurities. The impurities have an unintended effect on the final product [3,4]. The impurities in Ti scraps can act as substitutional or interstitial solid solutions in the final product. The impurities contaminated by deterioration or contained in the scraps can be removed through hydrogen plasma arc melting (HPAM). Pure titanium, titanium-based alloys, and high-value added pure metals can be purified through HPAM by adding hydrogen to the argon-plasma-generating gas [5,6]. It is one of the methods for an efficient removal of impurities forming a substitutional/interstitial solid solution through the high temperature and reactivity with hydrogen.

In this study, the effect of impurities in the $Fe_{29.5}Ti_{70.5}$ alloy prepared using Ti scraps was investigated. The Ti scraps were pretreated by washing with an ultrasonic cleaner in an alkaline degreasing solution and drying. The pretreated scraps were prepared into $Fe_{29.5}Ti_{70.5}$ ingots with Fe sources and refined for different times. The refined ingots were annealed at 1000°C for 5 hrs. After annealing, the effects of the impurities on the mechanical properties were evaluated through compression test.

2. Experimental

Ti scraps were washed through ultrasonic cleaning in a 10 g/L tetra-sodium pyrophosphate (TSPP) solution. The washed scraps were dried at 300°C for 30 minutes to complete the pretreatment. The base alloy was prepared through tilt casting in argon atmosphere using pretreated Ti scraps and Fe source. 30 g of the prepared base alloy was placed on a water-cooled copper mold, and the chamber was exhausted to 5.5×10^{-3} torr, and then ultra-high purity argon (99.9999%) and hydrogen (99.999%) were filled to atmospheric pressure at a rate of 12.5 L/min. The hydrogen content of the plasma gas was injected at 20 vol%, discharged at 8 kW, and melted for 5, 10, 15 minutes to prepared a button-type ingot. For uniform refining, the button-type ingot was turned upside down to repeat the previous melting. Then, ingots with a total melting time of 10, 20, 30 minutes were prepared. After HPAM was completed, the internal hydrogen was removed by PAM for 1 minute. The prepared ingots were an-

[1] JEONBUK NATIONAL UNIVERSITY, DIVISION OF ADVANCED MATERIALS ENGINEERING, COLLEGE OF ENGINEERING, JEONJU 54896, REPUBLIC OF KOREA
[2] KOREA BASIC SCIENCE INSTITUTE, DIVISION OF EARTH AND ENVIRONMENTAL SCIENCE, CHEONGJU 28119, REPUBLIC OF KOREA

* Corresponding author: jwlim@jbnu.ac.kr

nealed in a vacuum atmosphere at 1000°C for 5 hours to improve the microstructure, followed by furnace cooling.

In characterizations, XRD was performed on an X-ray diffractometer (Shimadzu, XRD-6100) in the step scan mode using Cu-Ka X-rays with a step size = 0.01° and 3-second count time per step over 30°-80° 2-theta. The substitutional impurity concentrations were determined using glow discharge mass spectrometry (GDMS, MSI, GD90). The oxygen, nitrogen, and carbon analyses (Eltra CS-2000, ON-900) were performed to determine the concentration of gas impurities. And, a cylindrical specimen having a diameter of 3 mm and height of 6 mm was prepared to evaluate the mechanical properties. The cylindrical specimen was subjected to a compression test at a speed of 1 mm/min using a universal testing machine (MTDI, UT-100). To understand the deformation behavior of the prepared alloy, a fracture surface of the specimen was analyzed using field-emission scanning electron microscopy (FE-SEM) and energy-dispersive spectroscopy (EDS) (Hitachi, SU-70).

3. Results and discussion

Figure 1, shows XRD patterns to evaluate the phase changes with the refining time (after HPAM of the $Fe_{29.5}Ti_{70.5}$ alloy) the main diffraction peaks of the alloys correspond to the body-centered cubic (BCC) β-Ti, a B2 FeTi intermetallic compound. Notably, no change in the peak was observed with the increase in HPAM time. Therefore, the removal of impurities by the refining did not have a significant effect on the phase; only the internal impurities were removed. However, in the sample of ingot (Just Annealed, HPAM 10 min), a small peak was observed around 42°, which is probably $Ti_4Fe_2O_{0.4}$. It appears to have reacted with oxygen in the initial incomplete chamber. As a result, it was then removed as the HPAM time increased.

$$Pi = r_i^0 N_i P_i^0 \tag{1}$$

Where r_i^0, N_i, and P_i^0 are the activity coefficients, moral fractions, and pure vapor pressures, respectively. The vapor pressures of various element have been reported [7]. The impurities can be easily removed as most of them have higher pure vapor pressures than that of the matrix Fe or Ti. The vapor pressure increases with the temperature, which facilitates the removal. When hydrogen was added to the argon plasma gas, the surface temperature increased by 300-400 K as hydrogen has a higher thermal conductivity than that of argon. The dissociated hydrogen can act as a carrier for the removal by reacting with metallic vapor [8].

$$xM(vap) + yH = M_xH_y(g)\uparrow \tag{2}$$

Interstitial elements such as oxygen, nitrogen, and carbon can also be removed by refining. These elements can be removed by combining with elements with higher affinities than that of Ti to form a compound [9].

$$xM(in\ molten\ metal) + \\ + yO(in\ molten\ metal) = M_xO_y(g)\uparrow \tag{3}$$

$$O(in\ molten\ metal) + \\ + H(from\ plasma\ gas) = H_xO(g)\uparrow \tag{4}$$

$$C(in\ molten\ metal) + \\ + zO(in\ molten\ metal) = CO_z(g)\uparrow$$

It can be assumed that the metallic/nonmetallic impurities were substitutional solid-solution-forming impurities with elements excluding H, C, N, and O, which are interstitial solid-solution-forming impurities. Figure 2 shows the change in concentration of impurities with the refining time. The content of impurities decreased with the increase in refining time. The impurities concentration of the initial ingot was 6733 ppm (substitutional impurities: 1704, interstitial solid-solution: 5029 ppm). After that, as the HPAM time increased, the impurities concentration was decreased. Finally, in the ingot by HPAM 30 min, the impurities concentration was decreased to 4573 ppm (substitutional impurities: 820, interstitial solid-solution: 3753 ppm).

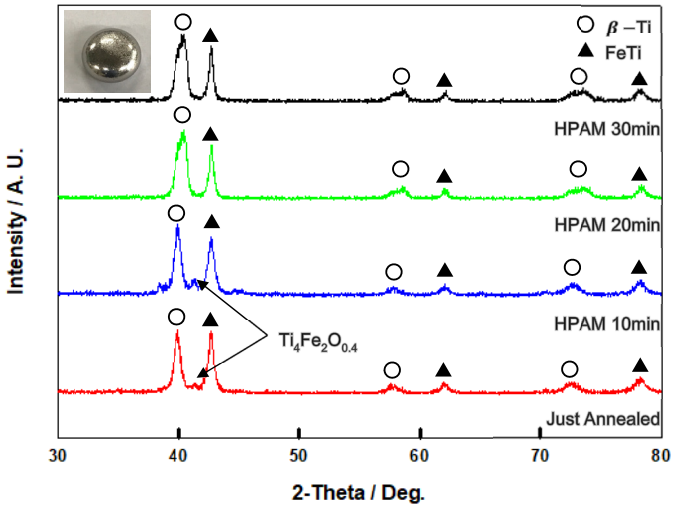

Fig. 1. XRD analyses of the $Fe_{29.5}Ti_{70.5}$ ingots refined for different times (10, 20, and 30 min)

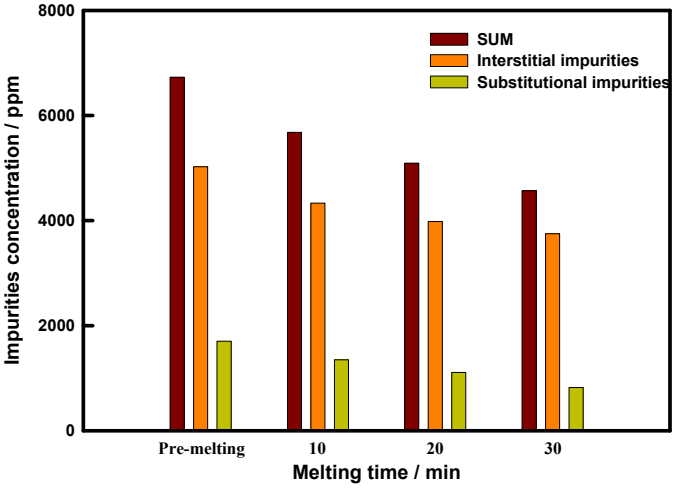

Fig. 2. Changes in concentration of impurities in the $Fe_{29.5}Ti_{70.5}$ ingot forming interstitial or substitutional solid solution as a function of the refining time

SEM images of the 30-min HPAM ingot are shown in Fig. 3. to evaluate the phase and composition changes of the microstructure upon the spheroidizing annealing. Figures 3(a)-3(e) confirm the lamellar structure of the ingot before the annealing. The interlayer spacing was on the nanometer scale. We expect that the high energy accumulated inside acted as a driving force during the heat treatment. Images after the annealing are shown in Figs. 3(f)-3(j). Coarse and spherical grain boundaries were observed. The matrix was β-Ti with a large Ti fraction, while the precipitation was FeTi. The FeTi has a simple cubic structure, whereas the β-Ti has a BCC structure, so that oxygen is more likely to penetrate the spaces between the lattices and thus has a higher solubility. Accordingly, more oxygen was observed in the β-Ti phase than in the FeTi phase (abundant red color).

TABLE 1

Room-temperature compression test results for the Fe29.5Ti70.5 alloys: Young's modulus E, yield stress σ_y, yield strain ε_y, ultimate compression stress σ_{max}, and fracture strain ε_f

Melting time	E (GPa)	σ_y (MPa)	ε_y (%)	σ_{max} (MPa)	ε_f (%)
Pre-melting	39.5	1802	4.8	1923	6.5
10 min	36.6	1719	4.9	1910	8.3
20 min	32.8	1635	5.2	1894	9.6
30 min	30.7	1563	5.3	1877	11.2

Compression tests were performed to evaluate the mechanical properties. The compressed specimens consisted of the annealed $Fe_{29.5}Ti_{70.5}$ ingots in cylindrical shapes with diameters of 3 mm and heights of 6 mm. The result of room-temperature

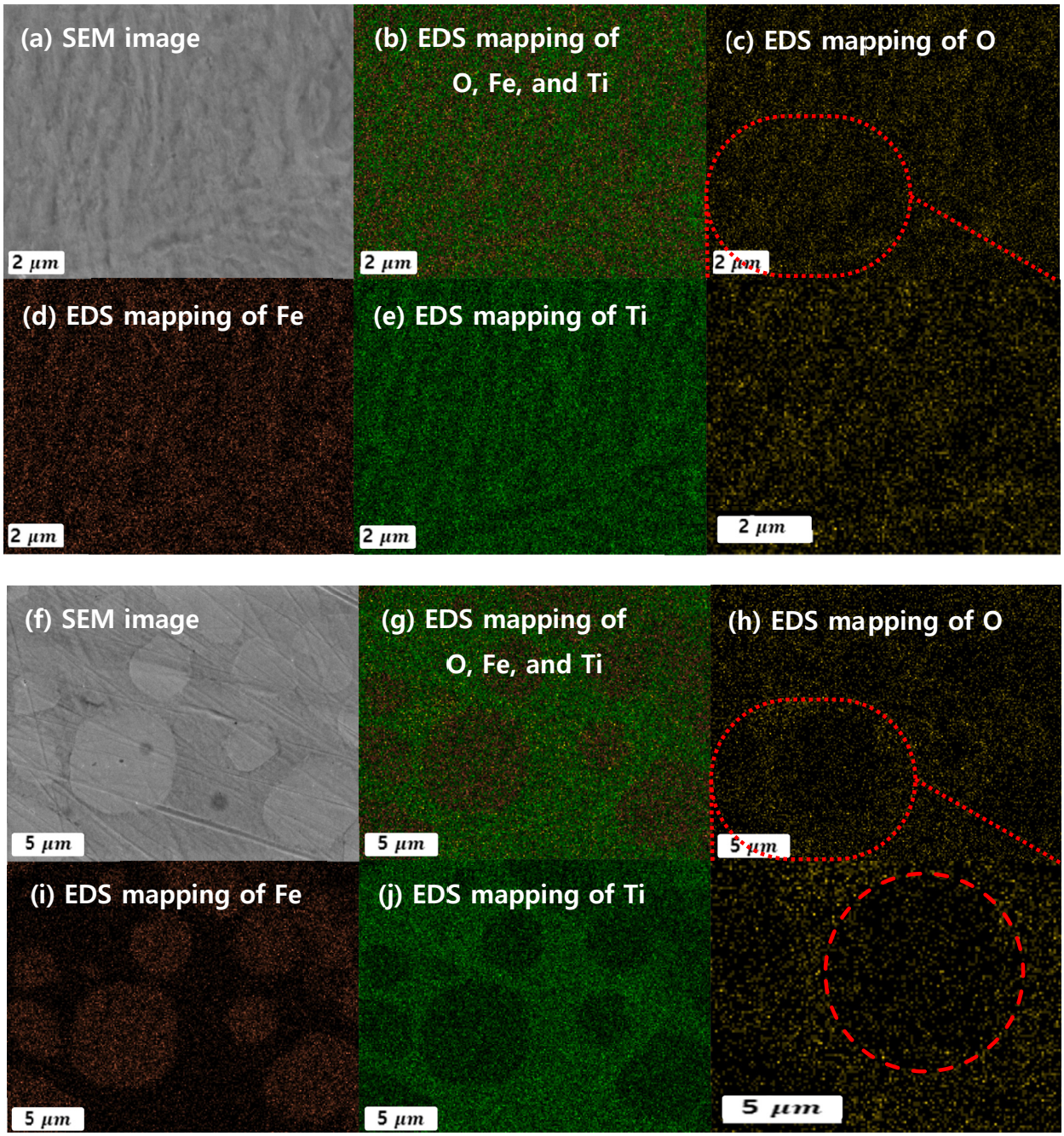

Fig. 3. SEM images of the $Fe_{29.5}Ti_{70.5}$ ingots refined for 30 min by the HPAM (a) before and (b) after the annealing

compressive test is shown in Table. 1. The three heat-treated compressed specimens were equal except for their impurity concentrations determined by the refining time. The Young's modulus of the nonannealed $Fe_{29.5}Ti_{70.5}$ alloy was approximately 95 GPa, whereas the Young's modulus of the grain was reduced owing to the spheroidization and coarsening [10]. However, when the annealing was not performed, the strain was improved compared to that at the strain of 2% appropriately. Notably, not only the Young's modulus, an intrinsic property of the material, but also the yield strength and strain were changed. Work hardening occurred upon the specimen compression, owing to the hindered dislocation movement and generation in the crystal structure. The impurities were located at the grain boundaries or became interstitial or substitutional solid solutions, which hindered the dislocation movement through the lattice distortion. Therefore, as the content of solid-solution-forming impurities decreased, the Young's modulus decreased from 36.6 to 30.7 GPa, the maximum yield stress decreased from 1910 to 1877 MPa, and the strain at fracture increased from 8.3 to 11.2.

Figure 4 shows the fracture surface of the specimen observed by SEM and EDS after the room-temperature compression test to investigate the fracture and deformation behavior of the alloy. Figures 4(a), 4(c), and 4(e) show wide areas of the cleavage fracture surfaces in the brittle material. With the increase in refining time, the content of impurities decreased and the cleavage surface tended to become fine. Figures 4(b), 4(d), and 4(f) show EDS images of the fracture surfaces. Notably, no precipitates such as oxides or carbides were observed. The FeTi phase, which has a relatively high Fe content, appears red with a clear shape, compared to the β-Ti phase, which is mainly

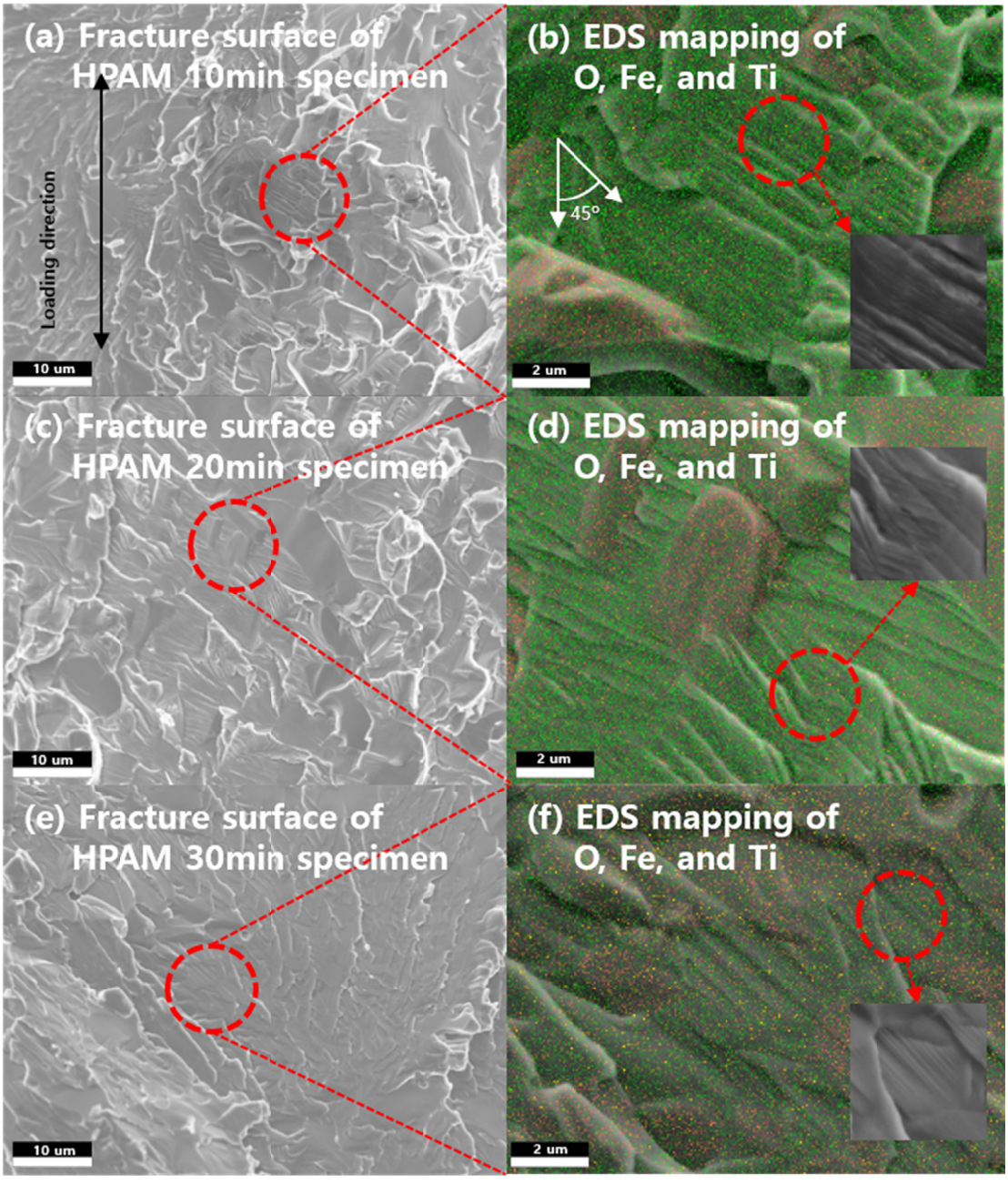

Fig. 4. SEM and EDS analyses of the fracture surfaces: (a)-(b) 10 min, (c)-(d) 20 min, and (e)-(f) 30 min HPAM, respectively

green. Thus, the relatively mild FeTi exhibited a grain boundary fracture. In β-Ti, a fine band was formed, inclined by approximately 45° in the load direction. Owing to this deformation band, the deformation occurred within β-Ti during the compression, which then fractured.

4. Conclusions

After the annealing of the $Fe_{29.5}Ti_{70.5}$ alloy ingots refined for different times by HPAM, their microstructures, compressive strengths, and fracture surfaces were analyzed. The content of impurities decreased with the increase in refining time. The impurities could form substitutional/interstitial solid solutions and affect the physical properties. The conclusions of this study can be summarized as follows.

(1) The contents of substitutional/interstitial solid-solution-forming impurities were reduced by 51.90 and 25.37 %, respectively, after the 30-min refining.

(2) Spheroidization and coarsening were achieved through the spheroidizing annealing and the strain was improved.

(3) The substitutional/interstitial solid-solution-forming impurities influenced the compression test results. With the decrease in content of impurities, the Young's modulus, yield stress, and ultimate compression stress decreased, while the strain increased.

(4) The analysis of fracture surface showed that the cleavage surface became finer with the decrease in content of impurities. The observed deformation band in β-Ti confirmed that the deformation and fracture occurred in β-Ti.

Acknowledgments

This study was supported by the Korea Institute of Energy Technology Evaluation and Planning and Ministry of Trade, Industry, and Energy of the Republic of Korea (No.20185210100030).

REFERENCES

[1] J.M. Park, D.H. Kim, K.B. Kim, N. Mattern, J. Eckert, J. Mater. Res. **26**, 365 (2011).

[2] M. Dao, L. Lu, R. Asaro, J.T. M. De Hosson, E. Ma, Acta Mater. **55**, 4041 (2007).

[3] K. Bensadok, S. Benammar, F. Lapicque, G. Nezzal, J. Hazard. Mater. **152**, 423 (2008).

[4] J. Chae, J.-M. Oh, S. Yoo, J.-W. Lim, Korean J. Met. Mater. **57**, 569 (2019).

[5] J.-M. Oh, K.-M. Roh, J.-W. Lim, J. Hydrog. Energy **41**, 23033 (2016).

[6] J.-M. Oh, B.-K. Lee, C.-Y. Suh, J.-W. Lim, J. Alloy. Compd. **574**, 1 (2013

[7] J.-W. Lim, G.-S. Choi, K. Mimura, M. Isshiki, Met. Mater. Int. **14**, 539 (2008).

[8] K. Mimura, S.-W. Lee, M. Ishiki, J. Alloy. Compd. **211**, 267 (1995).

[9] M.W. Chase Jr, W. Malcom, NIST-JANAF Thermochemical Table, 4th ed, J. Phys. Chem. Ref. Deta, Mohograph **9**, 154, 1537, 1759, 1776 (1995).

[10] J. Das, K. Kim, F. Baier, W. Löser, J. Eckert, Appl. Phys. Lett. **87**, 161907 (2005).